Emergence of a limit cycle for swimming microorganisms in a vortical flow of a viscoelastic fluid

A. M. Ardekani and E. Gore

Phys. Rev. E **85**, 056309 — Published 22 May 2012

DOI: 10.1103/PhysRevE.85.056309

Emergence of a limit cycle for swimming microorganisms in a vortical flow of a viscoelastic fluid

A.M. Ardekani and E. Gore
Aerospace and Mechanical Engineering,
University of Notre Dame,
Notre Dame, IN 46556, USA

We propose that the rheological properties of background fluid play an important role in the interaction of microorganisms with the flow field. The viscoelastic-induced migration of microorganisms in a vortical flow leads to the emergence of a limit cycle. The shape and formation rate of patterns depend on motility, the vorticity strength, and rheological properties of the background fluid. Given the inherent viscoelasticity of exopolysaccharides secreted by microorganisms, our results can suggest new mechanisms leading to the vital behavior of microorganisms such as bacterial aggregation and biofilm formation.

INTRODUCTION

Bacterial aggregation has several implications; it can lead to pathogen colonization and development of diseases and epidemics [1] and formation of biofilms [2]. It also affects ecological processes in aquatic environments such as development of patches of dissolved organic matter [3], nutrient turnover [4], and distribution of biomass in the ocean [5]. In marine environments, high concentrations of bacteria are present inside transparent exopolymer particles (TEP) [6], referred to as oceanic gel [7]. TEP presence is essential for the formation of diatom aggregates, the so-called "marine snow particles," that contribute to fluxes of carbon into the deep ocean [8]. In addition, TEP plays an important role in the biofilm initiation and fouling during membrane filtration processes (e.g. nanofilteration or reverse osmosis) [9]. Despite these widespread implications of the viscoelasticity of the microorganisms' habitats, their underlying hydrodynamics on the aggregation of bacteria and microorganisms are poorly understood at present.

Recent small-amplitude results of Taylor's infinite swimming sheet [10] suggest that viscoelasticity hinders locomotion [11]. On the other hand, an infinite swimming sheet in a Brinkmann fluid and two fluid gels shows increased swimming velocities [12, 13]. Both swimming velocity and mechanical efficiency are increased with viscoelasticity for a free finite sheet swimmer with large tail undulations. The peak corresponds to the relaxation time of the fluid matching the stroke frequency of the swimmer and is associated with regions of highly stressed fluid near the undulating tail [14]. In the case of a spherical squirmer in a complex fluid, the swimming velocity is found to be smaller than that in a Newtonian fluid, but the swimming efficiency increases with the liquid relaxation time [15]. Although propulsion of microorganisms in complex fluids has recently gained significant interest, other than the recent work on stability of suspension of microorganisms in a viscoelastic fluid [16], current studies have only considered the role of background fluid rheology on the propulsion of a single organism in stagnant flows (e.g. [11–13]). Therefore, more studies are required to understand the effect of non-Newtonian fluid properties on the interaction of microorganisms with the background flow. In this letter, we investigate the role of viscoelastic-induced migration of microorganisms in the presence of a vortical flow.

Recent experiments show that the presence of bacteria-produced extracellular polymeric substances (EPS) made of polysaccharides and proteins lead to aggregation of bacteria in curved microchannels under laminar flow regime and subsequently the formation of filamentous biofilm streamers [17]. Biofilm barriers are also developed in porous media to reduce the porosity, permeability, and mass transport in deep porous geological sites by several orders of magnitude and prevent leakage of CO_2 [18]. Inherently, vortical structures and secondary flows are present in porous media despite inertialess flows [19]. Control of the growth of biofilm in porous media and diagnostic microfluidic devices can be achieved with the knowledge of the background vortical flow and its effects on bacterial aggregation. We demonstrate that viscoelasticity of the background fluid in the presence of a vortical flow leads to the emergence of a limit cycle for swimming microorganisms that causes their aggregation. Aggregation patterns can be formed by various mechanisms such as gyrotaxis [5], density-dependent motility [20], and beating synchronization due to hydrodynamic interaction between microorganisms [21]. Here, we report a novel mechanism for microorganisms' pattern formation mediated by viscoelasticity of the background fluid.

MODEL

In order to quantify motion of microorganisms in the presence of flow, we proceed with a mathematical model to describe spatiotemporal evolution of the orientation

and trajectory of each microorganism [22]

$$\frac{d\mathbf{p}}{dt} = \frac{1}{2}\boldsymbol{\omega}\times\mathbf{p} + \frac{\gamma^2-1}{\gamma^2+1}\mathbf{p}\cdot\mathbf{E}\cdot[\mathbf{I}-\mathbf{pp}], \quad (1)$$

$$\frac{d\mathbf{x}_p}{dt} = V_s\mathbf{p} + \mathbf{u}(\mathbf{x}_p), \quad (2)$$

where each microorganism is modeled as a prolate spheroid of aspect ratio γ, swimming with a constant velocity, V_s, along direction $\mathbf{p}$. In these equations, t is time, $\boldsymbol{\omega}$ the background vorticity, $\mathbf{u}$ the background velocity field, $\mathbf{x}_p$ the particle position vector, $\mathbf{E} = (\boldsymbol{\nabla}\mathbf{u}+\boldsymbol{\nabla}\mathbf{u}^T)/2$ the rate of strain tensor, and $\mathbf{I}$ is the identity tensor. The orientation of elongated particles is affected by shear. Elongated spheroids undergo periodic rotation depending on their aspect ratio, called Jeffery orbit, [23] which is described by Eq. (1). The above equations have been widely used to model self-propulsion of particles and phytoplankton (e.g. [5, 22, 24]). Microorganisms swimming in extracellular polymeric substances are subjected to lateral migration across streamlines due to viscoelasticity of EPS which is not captured in Eqs. (1) and (2). Lateral migration in non-Newtonian fluids occurs due to the normal stress coefficients. These nonlinear elastic properties of complex fluids can lead to flow phenomena in contrast with their counterpart in Newtonian fluids. Rod climbing effects [25], elastic instabilities in inertialess flows [26], and microstructure formation in concentrated suspensions of particles of polymeric liquids [27–29] are examples where normal stress difference can significantly affect the flow. For a simple shear flow $u_x = \dot{\gamma}y$, first and second normal stress differences are defined as $N_1 = \sigma_{xx} - \sigma_{yy} = \psi_1\dot{\gamma}^2$ and $N_2 = \sigma_{yy} - \sigma_{zz} = \psi_2\dot{\gamma}^2$, where $\dot{\gamma}$ is the magnitude of shear rate and ψ_1, ψ_2 are the first and second normal stress coefficients which are zero for Newtonian fluids. For polymeric liquids, the first normal stress coefficient is positive but the second normal stress coefficient is negative. The lateral cross stream migration velocity can be described as a function of first and second normal stress coefficients. The second-order fluid is perhaps the simplest model to use for explicit analysis of normal and extensional stresses and has been widely used for analysis of particle motion in viscoelastic fluids [30, 31]. The stress tensor for a second-order fluid can be written as:

$$\mathbf{T} = -p\mathbf{I} + \eta_0\mathbf{A}_1 - \frac{1}{2}\psi_1\mathbf{A}_2 + (\psi_1+\psi_2)\mathbf{A}_1^2, \quad (3)$$

where η_0 is zero shear viscosity; $\mathbf{A}_1 = \boldsymbol{\nabla}\mathbf{u}+\boldsymbol{\nabla}\mathbf{u}^T$ is twice the strain rate tensor and

$$\mathbf{A}_2 = \frac{\partial\mathbf{A}_1}{\partial t} + (\mathbf{u}\cdot\boldsymbol{\nabla})\mathbf{A}_1 + \mathbf{A}_1\boldsymbol{\nabla}\mathbf{u} + \boldsymbol{\nabla}\mathbf{u}^T\mathbf{A}_1. \quad (4)$$

The undisturbed flow field can be locally expanded around location, $\mathbf{x}_p$, in a Taylor series as

$$\mathbf{u}(\mathbf{x}) = \boldsymbol{\alpha}(\mathbf{x}_p) + \mathbf{E}(\mathbf{x}_p)\cdot(\mathbf{x}-\mathbf{x}_p) + \boldsymbol{\chi}(\mathbf{x}_p):(\mathbf{x}-\mathbf{x}_p)(\mathbf{x}-\mathbf{x}_p) + h.o.t. \quad (5)$$

Here, we can assume that the presence of microorganisms does not modify the background flow field since the size of the microorganisms (O(1-10)μm) is much smaller than the length scale corresponding to the vortical structures in the background flow field. In addition, velocity fluctuations produced by microorganisms' collective behavior is on the order of O(10-100 μm/s) and is much smaller than the background velocity field. Chan and Leal [32] described viscoelasticity-induced lateral migration velocity, $\mathbf{V}_E$, of a sphere of radius a in a second-order fluid of general quadratic flow described by Eq. (5) as

$$\mathbf{V}_E = 2a^2\frac{\psi_1+\psi_2}{\eta_0}\left\{\frac{5}{18}(5+13\epsilon_1)\mathbf{E}:\boldsymbol{\xi} + \frac{1}{27}(1+11\epsilon_1)\boldsymbol{\varepsilon}:(\mathbf{E}\cdot\boldsymbol{\theta}) + \frac{1}{3}(1+3\epsilon_1)\mathbf{E}\cdot\boldsymbol{\tau}\right\}, \quad (6)$$

where $\epsilon_1 = -\frac{1}{2}(1+\psi_2/\psi_1)^{-1}$ and in component notation

$$\xi_{ijk} = \frac{1}{6}(\chi_{ijk}+\chi_{ikj}+\chi_{kij}+\chi_{kji}+\chi_{jik}+\chi_{jki}) - \frac{1}{15}(\chi_{imm}\delta_{jk}+\chi_{jmm}\delta_{ik}+\chi_{kmm}\delta_{ij}), \quad (7)$$

$$\theta_{ij} = \varepsilon_{imn}\chi_{nmj} + \varepsilon_{jmn}\chi_{nmi}, \quad \text{and} \quad \tau_i = \chi_{imm}, \quad (8)$$

where $\boldsymbol{\varepsilon}$ is the permutation tensor also known as the Levi-Civita tensor. The second normal stress coefficient ψ_2 is usually much smaller than ψ_1 and we neglect it in our analysis. The migration velocity of an ellipsoid in a simple shear flow of a second-order fluid is the same as for a sphere [33]. However, detailed numerical simulation of the nonlinear equations is needed to calculate the lateral viscoelastic-induced migration velocity of an ellipsoid in an inhomogeneous background flow (e.g. quadratic flow).

Next, we justify the use of Eq. (1) for non-Newtonian fluids. A transversely isotropic particle in a simple shear flow of a Newtonian fluid rotates indefinitely on one of an infinite, one-parameter family of Jeffery orbits [30]. There is no preferred orbit due to the "indeterminacy" of the Stokes' flow solution. Non-Newtonian behavior of EPS, however, breaks the symmetry [30]. Non-spherical axisymmetric particles in viscoelastic fluids show steady drift to a preferred orbit that depends on the particle aspect ratio. Slender prolate particles drift to the orbit in which the axis of rotation is parallel to the undisturbed vorticity vector [30, 33]. The rate of drift, however, depends on the magnitude of the rheological parameter, $(\psi_1+\psi_2)\dot{\gamma}(1+2\epsilon_1)/\eta_0$, as well as the detailed geometry of the particles. For spherical particles, the rate of rotation of particles in a non-Newtonian fluid remains the same as the one in a Newtonian fluid ($\frac{1}{2}\boldsymbol{\omega}\times\mathbf{p}$) independent of the value of the second normal stress coefficient. Thus, the rate of orbit drift is nonzero for elongated ellipsoids only in a fluid that exhibits a nonzero second normal stress, which is usually small. It should be noted that the orbit drift is different from viscoelastic-induced migration

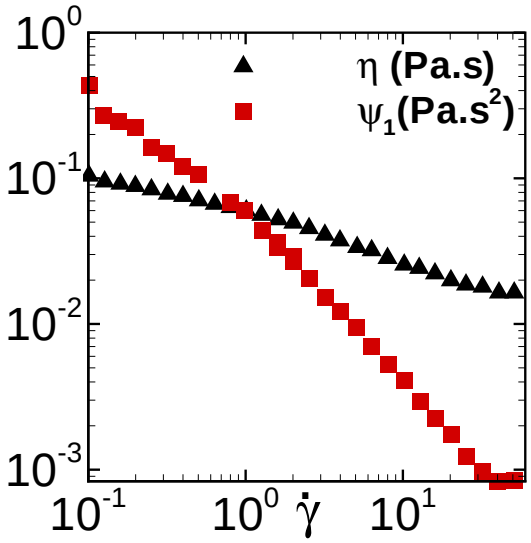

FIG. 1: (Color online) Viscosity and first normal stress coefficient are calculated for EPS of *Pseudomonas aeruginosa* biofilm using Cox-Merz [36] and Laun's [37, 38] rules for the data provided by Wloka *et al.* [34]

of particles across streamlines which is described by Eqs. (6)-(8) and occurs for both spherical and elongated objects in any viscoelastic fluids. In reality microorganisms may not be transversely isotropic. In that case, Eq. (1) should be modified to address the role of anisotropy of the microorganism on the Jeffrey orbit. However, detailed numerical calculation of the nonlinear equations is needed to explore the effect of viscoelasticity of the background fluid on the orbit drift of non-transversely isotropic particles, which is outside the scope of this paper.

Based on the discussion above, orientation and trajectory of each microorganism in the extracellular matrix can be written in dimensionless form as

$$\frac{d\mathbf{p}}{d\tilde{t}} = \frac{1}{2}\tilde{\boldsymbol{\omega}} \times \mathbf{p} + \frac{\gamma^2 - 1}{\gamma^2 + 1}\mathbf{p} \cdot \tilde{\mathbf{E}} \cdot [\mathbf{I} - \mathbf{pp}], \tag{9}$$

$$\frac{d\tilde{\mathbf{x}_p}}{d\tilde{t}} = \phi\mathbf{p} + \tilde{\mathbf{u}}(\tilde{\mathbf{x}_p}) + \tilde{\mathbf{V}}_E, \tag{10}$$

where $\sim$ refers to the dimensionless variables. Here, length and vorticity are scaled by L and ω_0, the representative length scale and vorticity scale of the background flow field, respectively. ϕ is the dimensionless swimming velocity, $\phi = V_s/L\omega_0$.

RESULTS AND DISCUSSION

In order to examine the role of rheological properties of the background fluid in a vortical flow, we consider a steady incompressible laminar flow field of a Taylor-Green vortex (TGV). The TGV flow, which consists of an array of counterrotating vortices, is given as $\mathbf{u} = \omega_0[-\cos mx \sin mz/2, 0, \sin mx \cos mz/2]$. Here, ω_0 is the maximum vorticity and L is taken to be $L = 1/m$. Using TGV as the background velocity field, the migration velocity in dimensionless form can be written as

$$\tilde{\mathbf{V}}_E = -0.194\tilde{a}^2\, Wi \sin\tilde{x} \sin\tilde{z} \begin{pmatrix} \cos\tilde{x}\sin\tilde{z} \\ 0 \\ \sin\tilde{x}\cos\tilde{z} \end{pmatrix}, \tag{11}$$

where $Wi = \lambda\omega_0$ is the Weissenberg number and $\lambda = \psi_1/2\eta_0$ the relaxation time of the liquid. Wloka *et al.* [34] measured rheological properties of extracellular polymeric substances for *Pseudomonas aeruginosa* biofilm. They reported concentration of dissolved polymer chains as 1.12 g/l with average molecular weight of $2,370,000$ g/mol and measured relaxation time of 17 ms. The volume fraction of bacteria within the biofilm is less than 0.2, and elasticity of the biofilm is essentially determined by the rheological properties of EPS (shown in Fig. 1) [35]. TEP assembles to form gels sparsely distributed in the bulk of the ocean but they can be locally found in higher concentrations (e.g. in diatoms blooms, or at the entrance of filtration membranes where they lead to biofilm initiation [9]). The use of a second-order fluid is the first step toward understanding the interaction of microorganisms and flow field in background fluids that obey a more complicated constitutive relation. In a second order fluid, the viscosity and normal stress coefficients are constant, whereas viscosity and normal stress coefficients are shear thinning for EPS of *Pseudomonas aeruginosa* biofilm as shown in Fig. (1). The basic mechanism explained in this paper is due to the presence of the normal stress difference which is also present in real polymeric fluids and extracellular polymeric substances. However, in order to quantitatively predict the rate of pattern formation for shear-thinning fluids, one needs to use other constitutive equations such as Giesekus or FENE-P models where fully nonlinear computational fluid dynamics calculations will be necessary. The results presented in this manuscript are quantitatively correct in the limit of low Weissenberg number but only provide a qualitative understanding in the limit of large Weissenberg number since transient effects of polymeric fluids are neglected in this work.

The size and magnitude of vortex structure in different applications are given as $L \sim O$(mm), $\omega_0 \sim O(10^{-4}$-$0.1\text{s}^{-1})$ in the ocean and $L \sim O$(10-100μm), $\omega_0 \sim O$(1-100 s^{-1}) near a small swimming organism, $L \sim O$(1-1000 μm) and $\omega_0 \sim O$(1-1000 $^{-1}$) in porous media, near membranes exposed to biofouling (e.g. nanofilteration or reverse osmosis) or diagnostic microfluidic devices. For $\tilde{a}$ $\sim$0.01-1 and Wi $\sim$0.1-100, the coefficient of lateral migration will be of order $\beta = 0.194\tilde{a}^2\, Wi \sim O(2 \times 10^{-6} - 20)$ where β is defined as $\beta = 0.194\tilde{a}^2\, Wi$.

The autonomous nonlinear dynamic system described

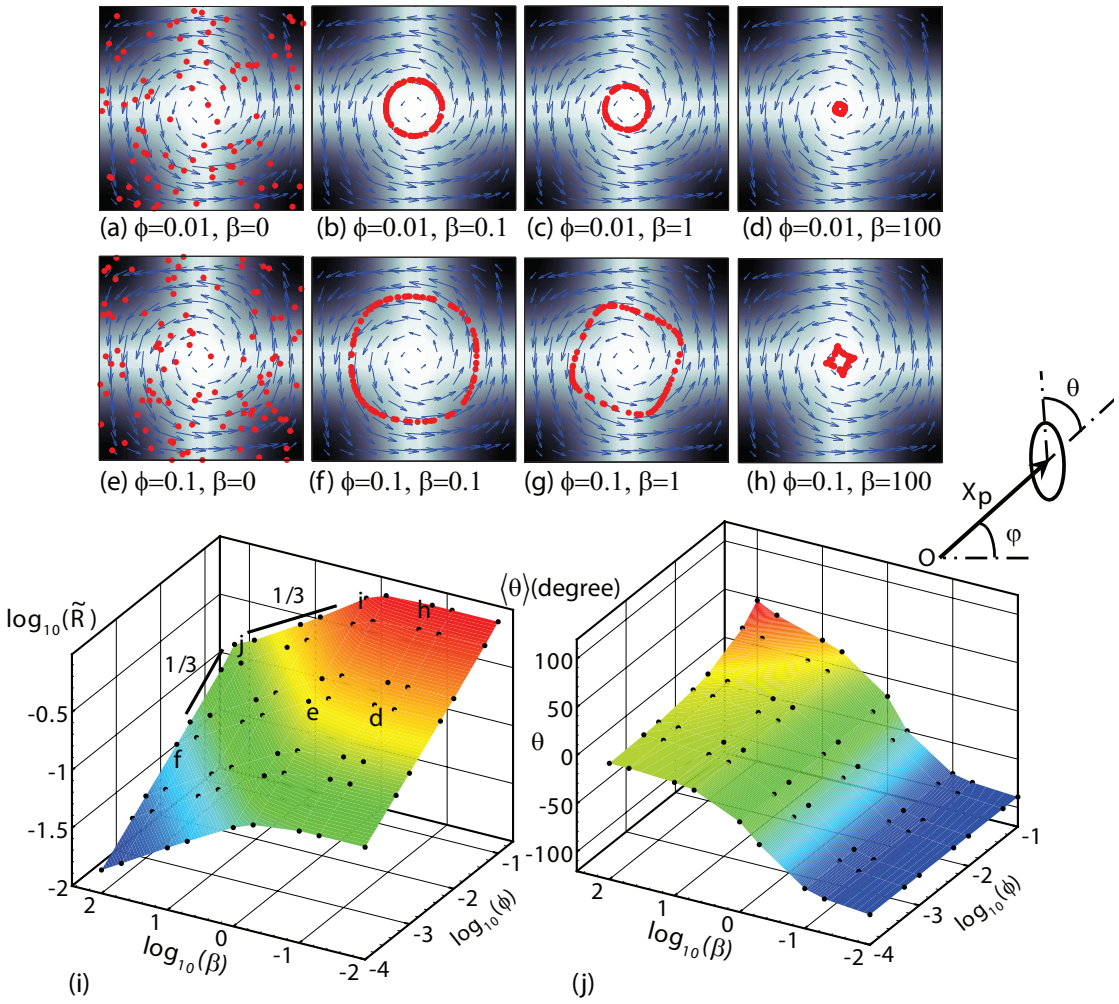

FIG. 2: (Color online) (a)-(h) Spatial distribution of microorganisms in Taylor-Green vortex of a viscoelastic fluid at $\gamma = 1$ for different values of motility and viscoelasticity are shown. The contours show the magnitude of shear rate tensor $\tilde{\dot{\gamma}} = \sqrt{2\tilde{\mathbf{E}} : \tilde{\mathbf{E}}} = |\sin\tilde{x}\sin\tilde{z}|$ and arrows represent velocity vectors for the background fluid. The size of the Taylor-Green cell is $\pi/2 \times \pi/2$ and dots represent bacteria. (i) Radius of the pattern and (j) orientation of microorganisms as a function of the dimensionless swimming velocity and viscoelasticity of the background fluid are plotted. The schematic shown in (j) illustrate polar angle and microorganism's orientation angle, where origin, O, is located at the center of the TGV cell.

by Eqs. (9-11) is numerically solved for 400 microorganisms using an explicit second-order time discritization scheme to rationalize the role of swimming velocity, background vorticity, and rheological properties of the background fluid. Each microorganism is initialized in space with random initial position and orientation. However as time evolves, microorganisms orbit in a limit cycle and eventually steady patterns emerge in the presence of viscoelasticity (see supplemental material movie 1 in [39]). Figure 2(a)-(h) shows microorganisms' pattern formation for different values of swimming velocity, ϕ, and fluid viscoelasticity, β. Viscoelasticity of the background fluid leads to migration of microorganisms towards region of low shear rate ($\tilde{\dot{\gamma}} = \sqrt{2\tilde{\mathbf{E}} : \tilde{\mathbf{E}}}$), which comes to balance with the motility of microorganisms at a particular radius leading to rotation of microorganisms on a periodic orbit. As microorganisms' motility increases, they have a stronger tendency to move on a straight line rather than as a passive tracer. This leads to formation of square shaped orbits (Fig. 2(f)-(h) and supplemental material movie 2 in [39]) rather than circular orbits ((Fig. 2(b)-(d)). The dynamical system describing microorganisms' trajectory and evolution (Eqs. (9-11)) has a limit cycle whose average radius, $\langle\tilde{R}\rangle$, depends on motility and viscoelasticity of the medium (Fig. 2(i)). Note that $\langle\rangle$ represents time average over a cycle. The angle θ is a measure of microorganism's orientation angle relative to the polar angle, φ, and is positive in counter-clockwise

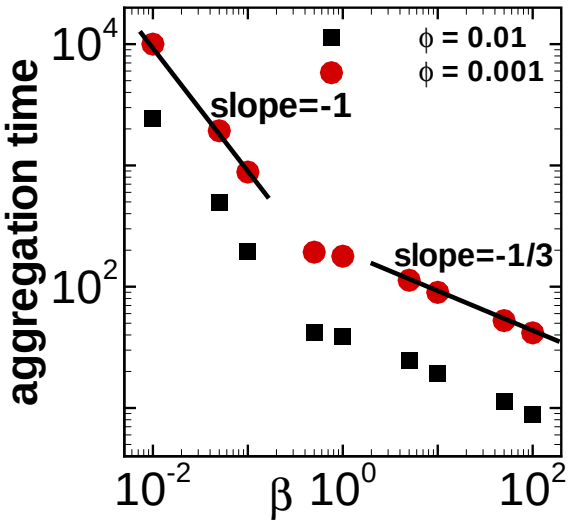

FIG. 3: (Color online) Aggregation time at which $\langle\tilde{R}\rangle$ reaches 90% of its steady value.

direction (see Fig. 2(j)). Microorganisms are oriented in a tangential direction as they rotate on the limit cycle for small values of β ($\langle\theta\rangle \to -\pi/2$) but oriented along radial direction as β increases (Fig. 2(j)). For large values of β, the dimensionless radius of the limit cycle is much smaller than unity and an analytical expression for it can be obtained after psuedo-linearization of Eqs. (9) and (10) around $\tilde{x} = 0$, $\tilde{z} = 0$:

$$\langle\dot{\tilde{R}}\rangle = -\frac{\beta}{4}\langle\tilde{R}\rangle^3 + \phi\cos\langle\theta\rangle \qquad (12)$$

where θ is a periodic function of φ, Fourier expansion of which can be written as $\theta = \langle\theta\rangle + A\cos(4\varphi + B) + h.o.t.$ When microorganisms are moving on the limit cycle, $\langle\dot{\tilde{R}}\rangle = 0$ and consequently, $\langle\tilde{R}\rangle = (4\phi\cos\langle\theta\rangle/\beta)^{1/3}$. This solution is also confirmed by numerical analysis shown in Fig. 2(i) where the radius of the limit cycle decays as $\beta^{-1/3}$ and increases as $\phi^{1/3}$ in the limit of large β. Aggregation rate of microorganisms is also controlled by their motility, strength of the vortical flow, and viscoelasticity of the background fluid. As shown in Fig. 3, aggregation rate increases with both ϕ and β. The higher the motility of microorganisms and the more viscoelastic the background fluid, the faster the limit cycle emerges. As microorganism's orbit approaches the limit cycle, the difference between $\langle\tilde{R}\rangle$ and average radius of the limit cycle, ϵ, becomes small compared to $\langle\tilde{R}\rangle$. Using Eq. (12) for large values of β, it can be easily shown that $d\epsilon/dt \propto \beta^{1/3}$. For small values of β, the radius of limit cycle is independent of β and Eqs. (10)-(11) can be used to show that $d\epsilon/dt \propto \beta$.

CONCLUDING REMARKS

In this letter, we analyze dilute suspension of non-interacting microorganisms and show that they trap within a vortex cell due to viscoelasticity of the background fluid. Particle trapping within the vortices driven by shear-induced migration has been reported in the literature [40]. Shear-induced migration velocity of a particle in a vortex scales as $U_{sh} \sim \dot{\gamma}a^2\phi_v/L$ where ϕ_v is the volume fraction of particles [41]. The ratio of shear-induced migration velocity relative to viscoelasticity-induced migration for microorganisms within a Taylor-Green vortex can be estimated as $U_{sh}/V_E \sim \phi_v/Wi$ which is small for bacteria suspensions and biofilms and is neglected in this analysis. The fundamental mechanism discussed in this paper, leading to the emergence of the limit cycle and eventually aggregation of microorganisms, is independent of their concentration. In fact, a single microorganism started at a random position and orientation will eventually rotate on a limit cycle as time passes. This is due to the fact that viscoelastic-induced migration, which leads to their motion to regions of low shear, balances with their motility, that acts as an opposing mechanism leading to their dispersion. The interaction of microorganisms with each other and their collective behavior can be neglected in this work since the microorganism concentration is low and the fluctuations generated by microorganisms are smaller than the background flow field.

Equations (1) and (2) for spherical self-propelled particles ($\gamma = 1$) do not predict any aggregation since the trace of Jacobian of Eqs. (1) and (2) is zero (due to incompressibility condition). Thus, "according to Liouville's theorem, there can be no contraction in phase space volume"[24] and no limit cycle occurs for spherical microorganisms in Newtonian fluids. On the other hand, considering viscoelasticity of the background fluid leads to motion of microorganisms on periodic orbits within a single vortex cell. These results await and invite experimental verification with natural or artificial swimmers [42]. The mechanism proposed here suggests that patches of bacteria and microorganisms form in the presence of vorticity due to elastic properties of extracellular polymers and can be used to generate large enough concentrations of microorganisms required for detection procedures. Detection of microorganisms such as bacteria is important in medical diagnosis, microbiological analysis of food, water and environmental samples.

ACKNOWLEDGMENTS

This work is supported by NSF grant CBET-1150348-CAREER. We are grateful to S.H. Yazdi for valuable discussions. We thank H.C. Chang, J. Powers, M. Sen, S.H. Yazdi for comments on an earlier version of this manuscript.

[1] J. Costerton, P. Stewart, and E. Greenberg, Science **284**, 1318 (1999).
[2] I. Klapper and J. Dockery, SIAM Review **52**, 221 (2010).
[3] F. Azam, Science **280**, 694 (1998).
[4] N. Blackburn, T. Fenchel, and J. Mitchell, Science **282**, 2254 (1998).
[5] W. M. Durham, E. Climent, and R. Stocker, Phys. Rev. Lett. **106**, 238102 (2011).
[6] P. Verdugo and P. Santschi, Deep Sea Res. Part II **57**, 1486 (2010).
[7] A. Alldredge, U. Passow, and B. Logan, Deep-Sea Res. Pt I **40**, 1131 (1993).
[8] D. Smith, M. Simon, A. Alldredge, and F. Azam, Nature **359**, 139 (1992).
[9] T. Berman, R. Mizrahi, and C. G. Dosoretz, Desalination **276**, 184 (2011)
.
[10] G. I. Taylor, Proc. R Soc. Lon. Ser-A **209**, 447 (1951).
[11] E. Lauga, Phys. Fluids **19**, 83 (2007).
[12] A. M. Leshansky, Phys. Rev. E **80**, 051911 (2009).
[13] H. C. Fu, V. B. Shenoy, and T. R. Powers, Europhys. Lett. **91**, 24002 (2010).
[14] J. Teran, L. Fauci, and M. J. Shelley, Phys. Rev. Lett. **104**, 038101 (2010).
[15] L. Zhu, M. Do-Quang, E. Lauga, and L. Brandt, Phys. Rev. E **83**, 011901 (2011).
[16] Y. Bozorgi and P. T. Underhill,Phys. Rev. E **84**, 061901 (2011).
[17] R. Rusconi, S. Lecuyer, L. Guglielmini, and H. Stone, J. R. Soc. Interface (2010).
[18] A. Mitchell, A. Phillips, R. Hiebert, R. Gerlach, L. Spangler, and A. Cunningham, Int. J. Greenh. Gas Con. **3** (2009).
[19] K. Vafai, *Porous Media: Applications in biological systems and Biotechnology* (CRC Press, Boca Raton, FL, 2011).
[20] M. Cates, D. Marenduzzo, I. Pagonabarraga, and Tailleur, PNAS **107**, 11715 (2010).
[21] I. Riedel, K. Kruse, and J. Howard, Science **309**, 300 (2005).
[22] T. Pedley and O. Kessler, Ann. Rev. Fluid Mech. **24**, 313 (1992).
[23] G. B. Jeffery, P. Roy. Soc. Lond. A Mat. **102**, 161 (1922).
[24] C. Torney and Z. Neufeld, Phys. Rev. Lett. **99**, 078101 (2007).
[25] F. Garner and A. Nissan, Nature **158**, 634 (1946).
[26] E. Shaqfeh, Ann. Rev. Fluid Mech. **28**, 129 (1996).
[27] G. McKinley, *"Steady and Transient Motion of a Sphere in an Elastic Fluid" in Transport Processes in Bubbles, Drops and Particles*, 2nd ed., edited by D. Kee and R. Chhabra (Taylor and Francis, New York, 2002).
[28] A. M. Ardekani, R. H. Rangel, and D. Joseph, Phys. Fluids **20**, 063101 (2008).
[29] A. M. Ardekani, D. Joseph, D. Dunn-Rankin, and R. H. Rangel, J. Fluid Mech. **633**, 475 (2009).
[30] L. Leal, J. non-Newton. Fluid **5**, 33 (1979).
[31] A. M. Ardekani, R. H. Rangel, and D. Joseph, J. Fluid Mech. **587**, 163 (2007).
[32] P. C. H. Chan and L. G. Leal, J. Fluid Mech. **82**, 549 (1977).
[33] P. Brunn, J. Fluid Mech **82**, 529 (1977).
[34] M. Wloka, H. Rehage, H. Flemming, and J. Wingender, Colloid. Polym. Sci. **282**, 10671076 (2004).
[35] J. Wilking, T. Angelini, A. Seminara, M. Brenner, and D. Weitz, MRS Bulletin **36**, 385 (2011).
[36] W. P. Cox and E. H. Merz, J. Polym. Sci. **28**, 619 (1958).
[37] H. M. Laun, J. Rheol. **30**, 459 (1986).
[38] V. Sharma and G. H. McKinley, Rheol. Acta (2012).
[39] See supplemental material at for movies.
[40] L. Yeo, D. Hou, S. Maheshswari, and H. Chang, Appl Phys Lett **88**, 233512 (2006).
[41] D. Leighton and A. Acrivos, J Fluid Mechanics **181**, 415 (1987).
[42] P. Tierno, R. Golestanian, I. Pagonabarraga, and F. Sagues, J Phys Chem B **112**, 16525 (2008).